Magnetic breakdown in metals: spin dynamics of conduction electrons

Yu. N. Proshin

S. M. Kirov Chemical-Technological Institute
(Submitted 13 February 1987)
Zh. Eksp. Teor. Fiz. **93**, 1356–1372 (October 1987)

We investigate interband magnetic breakdown (MB) in a metal with an arbitrary dispersion law, taking account of spin-orbit coupling and the spin splitting of conduction electron (CE) levels in a magnetic field. We determine the CE spectrum in regions of quasimomentum space having a small band gap. An expression is derived for the full fourth-rank s matrix, a fundamental dynamic characteristic of MB, and for the probability of MB with spin flip. As an example, we derive the dispersion relation and determine expressions for the CE g-factor in a simple "double figure eight" MB configuration, for various limiting cases. We demonstrate that just as in the case of stochastic MB, coherent MB can result in broadening of the CE paramagnetic resonance line in Zn and Mg.

1. The term "magnetic breakdown" [1] (MB) refers to a collection of phenomena due to tunneling of conduction electrons (CE) in a magnetic field between classical trajectories in different bands. The reviews in Refs. 2 and 3 give a fairly complete picuture of the work done in this field following the experimental discovery of MB in 1961.[1] A cornerstone of the theoretical treatment of MB is the ability to isolate small regions of quasimomentum space[3,4] within which CE wave functions from different bands overlap in a strong magnetic field, and the usual quasiclassical approximation for metals (see Ref. 5, for example) is inapplicable. Because these regions where two bands are anomalously close are small, it is possible to treat them as independent quantum scattering centers for conduction electrons, moving along quasiclassical trajectories in a magnetic field $\mathbf{H}(0,0,H)$:

$$\varepsilon_{m\rho}(\mathbf{p})=E, \qquad p_z=p_{z0}=\text{const}, \tag{1}$$

where E is the energy, $\varepsilon_{m\rho}(\mathbf{p})$ is the CE dispersion relation in the m-band, $\rho=\uparrow,\downarrow$ is the "spin" subscript, taking spin-orbit coupling (SOC) into account,[6,7] and $\mathbf{p}$ is the CE quasimomentum. We assume that the energy E lies in the range of band overlap:

$$\min\{\varepsilon_{2\rho}(\mathbf{p})\}<E<\max\{\varepsilon_{1\rho}(\mathbf{p})\}. \tag{1a}$$

One fundamental dynamic characteristic of MB is the scattering matrix or s-matrix,[3,4] which relates quasiclassical CE wave functions on segments of CE trajectories (1) in two bands which converge at a MB center. Knowing the elements of the s-matrix, it is easy to derive the probability of MB and of phase jumps in the CE wave function occurring during MB, to find the CE energy spectrum, and to calculate macroscopic electronic properties of a metal under MB conditions.[3,4,8,9] Up to now, the usual second-rank s-matrix obtained in Ref. 4, which is the same for all CE spin directions, has been used in MB theory. Thus, the theory has dealt with two independent types of CE motion under MB conditions, spin up and spin down.

Using a simple model of a metal, it was noted in Ref. 10 that SOC can lead to CE spin flip during MB. Thus, the s-matrix can have nonzero nondiagonal spin terms, and the addition of two spin degrees of freedom requires that a full fourth-rank s-matrix be calculated for a metal with arbitrary dispersion relation.

To find the s-matrix when SOC is present, we generalize the method of Ref. 4, in which spin was ignored in the derivation of the s-matrix elements. We first investigate the CE spectrum with no magnetic field, taking SOC into account, in regions of $\mathbf{p}$-space "suspected" of MB, with a band gap Δ which is much smaller than ε_0 (ε_0 is of the order of the width of the band). Then, after constructing the CE Hamiltonian for $H\neq 0$ in such a region (hereafter called an MB region) and solving the corresponding Schroedinger equation, we find the CE wave functions. Finally, by matching these functions and the quasiclassical wave functions which apply far from the MB regions, we obtain the full s-matrix.

Using the s-matrix thus obtained, we analyze the spectrum of a simple "figure eight" MB configuration, and find an expression for the electron g-factor of such a trajectory for various limiting cases.

As in Ref. 4, the calculations here are carried out to first order in $\varkappa=\hbar\omega_c/\varepsilon_0$, where ω_c is the characteristic cyclotron frequency of the conduction electron. This condition holds for $H\ll 10^8$–10^9 Oe, and does not in fact restrict the applicability of our results.

2. Let us consider the CE spectrum for $H=0$, with spin-orbit coupling. We write the one-particle Schroedinger equation in the $\mathbf{p}$-representation[5–7]:

$$\hat{\mathcal{H}}(\mathbf{p})\,u_{m\mathbf{p}\rho}(\mathbf{r})=\varepsilon_{m\rho}(\mathbf{p})\,u_{m\mathbf{p}\rho}(\mathbf{r}),$$

$$\hat{\mathcal{H}}(\mathbf{p})=e^{-i\mathbf{p}\mathbf{r}/\hbar}\hat{\mathcal{H}}e^{i\mathbf{p}\mathbf{r}/\hbar}. \tag{2}$$

Here $\hat{\mathcal{H}}=\hat{\mathcal{H}}^0+\hat{\mathcal{H}}^s$ is the CE Hamiltonian with $H=0$, $\hat{\mathcal{H}}^s$ is the SOC Hamiltonian, and $\mathbf{p}$ enters into (2) as a parameter. In the presence of SOC, the Bloch factor $u_{m\rho\rho}$ for the stationary CE wave function

$$\Psi_{m\rho\rho}(\mathbf{r})=e^{i\mathbf{p}\mathbf{r}/\hbar}u_{m\rho\rho}(\mathbf{r})$$

becomes a spinor[6,11]:

$$u_{m\rho\rho}(\mathbf{r})=\begin{pmatrix}\lambda^{(m)}_{\mathbf{p}\rho}(\mathbf{r})\\ \mu^{(m)}_{\mathbf{p}\rho}(\mathbf{r})\end{pmatrix}, \tag{3}$$

where we assume[6] that $|\lambda_{\mathbf{p}\uparrow}|>|\mu_{\mathbf{p}\uparrow}|$, so that the eigenvalue $\hat{\sigma}_z$ of the Pauli spin matrix is greater than zero:

$$\langle\Psi_{m\mathbf{p}\uparrow}|\hat{\sigma}_z|\Psi_{m\mathbf{p}\uparrow}\rangle>0.$$

Since the lattices of all metals contain inversion centers,

 0038-5646/87/100770-10$04.00

for $H=0$ we have $\varepsilon_{m\uparrow}(\mathbf{p})=\varepsilon_{m\downarrow}(\mathbf{p})=\varepsilon_m(\mathbf{p})$, i.e., with SOC, the system of a two-fold "spin" degeneracy, and because of time-reversal symmetry, $\Psi_{mp\downarrow}$ is related to $\Psi_{mp\uparrow}$ by the conjugation operator $\hat{C}$ (Ref. 6):

$$\Psi_{mp\downarrow}=\pm\hat{C}\Psi_{mp\uparrow},\quad \Psi_{mp\uparrow}=\mp\hat{C}\Psi_{mp\downarrow},\quad \hat{C}=i\delta_y\hat{I}\hat{K}, \tag{4}$$

where $\hat{I}$ and $\hat{K}$ are the spatial inversion and complex conjugation operators, respectively. The sign of the result depends on the parity of the CE wave function: the upper sign holds for a wave function which is even at the center of the m-band, and the lower holds for an odd function.

It is well known[6,7] that the extent to which SOC affects the band spectrum and CE wave functions depends on the relationship between the coupling energy $\xi^{(m)}\ll\varepsilon_0$ and the distance to the nearest band in which SOC is neglected,

$$\Delta^0(\mathbf{p})=|\varepsilon_m{}^0(\mathbf{p})-\varepsilon_{m'}{}^0(\mathbf{p})|,\quad m\neq m',$$

where $\varepsilon_m^0(\mathbf{p})$ is the energy eigenvalue corresponding to $\hat{\mathscr{H}}^0(\mathbf{p})$. For example, when $\xi^{(m)}\ll\Delta^0(\mathbf{p})$, spin-orbit coupling has only a minor influence on the spectrum, and it can be assumed that the band gap is

$$\Delta(\mathbf{p})=|\varepsilon_m(\mathbf{p})-\varepsilon_{m'}(\mathbf{p})|\approx\Delta^0(\mathbf{p}).$$

For estimation purposes, we use $\Psi_{mp\rho}$ obtained from first-order perturbation theory (see, for example Refs. 7, 12):

$$\Psi_{mp\rho}=\Psi^0_{mp\rho}+\sum_{m'\neq m,\rho'}\frac{\langle m\rho|\hat{\mathscr{H}}^s|m'\rho'\rangle}{\varepsilon_{m\rho}{}^0(\mathbf{p})-\varepsilon^0_{m'\rho'}(\mathbf{p})}\Psi^0_{m'p\rho'}, \tag{5}$$

where $\Psi^0_{mp\rho}=\Psi^0_{mp}\chi^0_\rho$ is an eigenfunction of $\hat{\mathscr{H}}^0$, and χ^0_ρ is a pure spin function:

$$\chi_\uparrow{}^0=\begin{pmatrix}1\\0\end{pmatrix},\quad \chi_\downarrow{}^0=\begin{pmatrix}0\\1\end{pmatrix}.$$

Since SOC in a real metal is governed by regions deep within the ions,[13,14] we may replace the matrix element of $\mathscr{H}^s$ in the Bloch functions, for our estimates, by the matrix element of the spin-orbit Hamiltonian between atomic wave function.[1)] To the indicated approximation, we then have from Eq. (5)

$$|\mu_{p\uparrow}/\lambda_{p\uparrow}|\approx\xi/\Delta(\mathbf{p}). \tag{6}$$

It can thus be seen that when $\Delta(\mathbf{p})\approx\varepsilon_0$, spin-orbit coupling can be ignored.

In order to find $\lambda_{\mathbf{p}\uparrow}$ and $\mu_{\mathbf{p}\uparrow}$ when $\xi\approx\Delta^0(\mathbf{p})$, it is generally necessary to solve the appropriate secular equation.[7,12,14,15] We note in passing that $\mu_{\mathbf{p}\uparrow}$ can become of order $\lambda_{\mathbf{p}\uparrow}$, and when $\Delta^0(\mathbf{p})=0$, the degeneracy can be removed by spin-orbit coupling,[7,14,15] i.e., $\Delta(\mathbf{p})\neq0$.

The close approach of trajectories (1) having different indices m occurs in those regions of $\mathbf{p}$-space where the band gap satisfies $\Delta(\mathbf{p})\ll\varepsilon_0$. It is clear from the foregoing estimates that SOC can have an important effect in such regions on CE wave functions and the structure of the band spectrum.

We now take a more detailed look at the CE spectrum in the presence of SOC and with $H=0$, in the vicinity of some point $\mathbf{p}'$ at which two bands approach one another closely and $\Delta(\mathbf{p})\ll\varepsilon_0$. Since for given $\mathbf{p}'$, the $u_{mp'\rho}(\mathbf{r})$ comprise a complete set of orthonormal functions, they can be used to expand $u_{mp\rho}$ at any other point $\mathbf{p}$:

$$u_{mp\rho}=\sum_{m'\rho'}R_{m\rho,m'\rho'}(\mathbf{p}|\mathbf{p}')u_{m'p'\rho'},$$

$$R_{m\rho,\,m'\rho'}(\mathbf{p}|\mathbf{p}')=\langle u_{m'p'\rho'}|u_{mp\rho}\rangle. \tag{7}$$

In a small neighborhood of $\mathbf{p}'(\delta\mathbf{p}=\mathbf{p}-\mathbf{p}',\ |\delta\mathbf{p}|\ll G$, where G is the characteristic period in $\mathbf{p}$-space), the influence exerted by other bands can be neglected[4]:

$$R_{m\rho,\,m'\rho'}(\mathbf{p}|\mathbf{p}')\sim1\quad(m,\,m'=1,2),$$
$$R_{m\rho,\,m'\rho'}(\mathbf{p}|\mathbf{p}')\approx O(|\delta\mathbf{p}|/G)\quad(m,\,m'\neq1,2). \tag{8}$$

For the sake of definiteness, we assume from here on that the two anomalously nearby bands have indices $m=1$ and $m=2$.

Taking advantage of the smallness of $\delta\mathbf{p}$, we obtain the following expansion from Eq. (2):

$$\hat{\mathscr{H}}(\mathbf{p})=\hat{\mathscr{H}}(\mathbf{p}')+\hat{\mathbf{V}}(\mathbf{p}')\delta\mathbf{p}+O[(|\delta\mathbf{p}|/G)^2], \tag{9}$$

where

$$\hat{\mathbf{V}}(\mathbf{p})=e^{-i\mathbf{pr}/\hbar}\hat{\mathbf{V}}e^{i\mathbf{pr}/\hbar},\quad \hat{\mathbf{V}}=\frac{i}{\hbar}[\hat{\mathscr{H}},\hat{\mathbf{r}}]=\frac{\hat{\mathbf{p}}}{m}+\frac{i}{\hbar}[\hat{\mathscr{H}}^s,\hat{\mathbf{r}}], \tag{9a}$$

and $\hat{\mathbf{V}}$ is the CE velocity operator with $H=0$. Substituting (7) and (9) into the Schroedinger equation (2) and making use of (8), we obtain a system of four equations:

$$\sum_{m'\rho'}\{[\varepsilon_{m'\rho'}(\mathbf{p}')-E]\delta_{m'm''}\delta_{\rho'\rho''}+\mathbf{V}_{m''\rho'',\,m'\rho'}(\mathbf{p}')\delta\mathbf{p}\}R_{m\rho,m'\rho'}(\mathbf{p}|\mathbf{p}')=0,$$

$$E=\varepsilon_{m\rho}(\mathbf{p}),\quad \mathbf{V}_{m\rho,\,m'\rho'}(\mathbf{p})=\langle u_{mp\rho}|\mathbf{V}(\mathbf{p})|u_{m'p\rho}\rangle,$$

$$m,\,m',\,m''=1,2. \tag{10}$$

Due to symmetry under the conjugation operation (4), the matrix $\hat{\mathbf{V}}(\mathbf{p})$ appears as follows:

$$\hat{\mathbf{V}}=\begin{pmatrix}\mathbf{V}_{1,1}(\mathbf{p}) & 0 & \mathbf{C}(\mathbf{p}) & \mathbf{D}(\mathbf{p})\\ 0 & \mathbf{V}_{1,1}(\mathbf{p}) & \mp\mathbf{D}(\mathbf{p}) & \pm\mathbf{C}(\mathbf{p})\\ \mathbf{C}(\mathbf{p}) & \mp\mathbf{D}(\mathbf{p}) & \mathbf{V}_{2,2}(\mathbf{p}) & 0\\ \mathbf{D}(\mathbf{p}) & \pm\mathbf{C}(\mathbf{p}) & 0 & \mathbf{V}_{2,2}(\mathbf{p})\end{pmatrix}, \tag{11}$$

where

$$\mathbf{V}_{m,m}=\mathbf{V}_{m\uparrow,\,m\uparrow}=\mathbf{V}_{m\downarrow,\,m\downarrow},\quad \mathbf{C}(\mathbf{p})=\mathbf{V}_{1\uparrow,\,2\uparrow}(\mathbf{p}),\quad \mathbf{D}(\mathbf{p})=\mathbf{V}_{1\uparrow,\,2\downarrow}(\mathbf{p}).$$

The upper signs apply when the wave functions in the two bands are of the same parity, and the lower signs apply otherwise. It can be shown, as in Ref. 4, that because of the invariance of $\hat{\mathscr{H}}$ under $\hat{I}$, phase factors can be chosen for the wave functions in such a way that $\operatorname{Im}\mathbf{C}(\mathbf{p})=\operatorname{Im}\mathbf{D}(\mathbf{p})=0$ for all points in $\mathbf{p}$-space. The difference between the present results and those in Ref. 4 is associated with the appearance of $\mathbf{D}\neq0$ in the matrix $\hat{\mathbf{V}}$ due to spin-orbit coupling. For $\mathbf{D}=0$, the matrix (11) can be decomposed into two independent second-rank matrices, and we arrive at the same results as in Ref. 4 for either spin direction. For $\xi\ll\Delta$, we can estimate the magnitude of $\mathbf{D}$. Using (5) and (6), we obtain for the main contribution [$\sim p/m$ in (9a)] $|\mathbf{D}(\mathbf{p})|\approx[\xi/\Delta(\mathbf{p})]V_0$,

where $V_0 \sim |\mathbf{V}_{m\rho,m\rho}|$ is the characteristic speed of the conduction electrons. For $\xi \gtrsim \Delta^0$, it can happen that $|\mathbf{D}| \sim V_0$.

Equating the determinant of the system (10) to zero, we find the CE spectrum near $\mathbf{p}'$; it is found to be doubly degenerate ($H = 0$):

$$\varepsilon_{1\rho,2\rho}(\mathbf{p}) = \frac{1}{2}\sum_m \varepsilon_m(\mathbf{p}') + \frac{1}{2}\sum_m \mathbf{V}_{m,m}(\mathbf{p}')\,\delta\mathbf{p}$$
$$\pm\{{}^1/_4[\Delta(\mathbf{p}') + B(\mathbf{p}')\delta\mathbf{p}]^2 + [\mathbf{C}(\mathbf{p}')\delta\mathbf{p}]^2 + (\mathbf{D}(\mathbf{p}')\delta\mathbf{p})^2\}^{1/2},$$
$$\mathbf{B} = \mathbf{V}_{1,1} - \mathbf{V}_{2,2}, \quad \Delta(\mathbf{p}') = \varepsilon_1(\mathbf{p}') - \varepsilon_2(\mathbf{p}'). \qquad (12)$$

The smallness of Δ in Eq. (12) means that in the neighborhood of $\mathbf{p}'$, the dispersion law $\varepsilon_{m\rho}(\mathbf{p})$ (and its corresponding Bloch factors) is a sharply peaked function of $\mathbf{p}$, i.e., it typically varies within an interval $\lesssim (\Delta/\varepsilon_0)G \ll G$ (considered in more detail in Ref. 4).

In order to analyze conduction electron behavior for $H \neq 0$, it is convenient in what follows to employ a modified Kohn-Luttinger representation.[4] To do so, we need functions which depend smoothly on at least one component of $\mathbf{p}$ (see Sec. 3). The $\varepsilon_{m\rho}(\tilde{\mathbf{p}})$ [and the corresponding $u_{m\tilde{\mathbf{p}}\rho}(\mathbf{r})$] are such functions, where $\tilde{\mathbf{p}}$ lies in a region of $\mathbf{p}$-space near $\mathbf{p}'$ in which $\Delta(\mathbf{p}) = \varepsilon_{1\rho}(\mathbf{p}) - \varepsilon_{2\rho}(\mathbf{p})$ attains a minimum [the $\varepsilon_{m\rho}(\mathbf{p})$ are given in Eq. (12)]:

$$\min \Delta(\mathbf{p}) = \Delta(\tilde{\mathbf{p}}).$$

There are generally no physical restrictions on the mutual orientation of the matrix elements of the CE velocity operator—the vectors $\mathbf{B}$, $\mathbf{C}$, and $\mathbf{D}$ in Eq. (12) [see also Eq. (11)]. In seeking a minimum of $\Delta(\mathbf{p})$, we therefore analyze all of the possible configurations.

1) The three vectors $\mathbf{B}$, $\mathbf{C}$, $\mathbf{D}$ in (12) are collinear: $\mathbf{B}(\mathbf{p}') \| \mathbf{C}(\mathbf{p}') \| \mathbf{D}(\mathbf{p}')$. Everywhere in the neighborhood of $\mathbf{p}'$, we then have $\Delta(\mathbf{p}) \neq 0$, and $\Delta(\mathbf{p})$ attains a minimum on the plane

$$\mathbf{B}\delta\mathbf{p} = -\Delta(\mathbf{p}')|\mathbf{B}|^2(|\mathbf{B}|^2 + 4|\mathbf{C}|^2 + 4|\mathbf{D}|^2)^{-1}$$

(called the M-plane from here on[4]). Because of the smallness of the pseudopotential for many metals, such spectra are common, and the M-plane coincides with the boundary of the Brillouin zone.[3,5,13,14] On this point, in Ref. 13, the smallness of the pseudopotential (narrower, however, than with SOC) is presented as an argument for the importance of SOC in the MB spectrum of Zn, Mg, and other hexagonal metals. Other mechanisms can also give rise to this type of spectrum.[3,4,16]

Near the M-plane, the dispersion relation is given by

$$\varepsilon_{1\rho,2\rho}(\mathbf{p}) = \frac{1}{2}\sum_m \varepsilon_m(\mathbf{p}_M) + \frac{1}{2}\sum_m V^{(n)}_{m,m}(\mathbf{p}_M)\,\delta p_n$$
$$\pm\left\{\frac{1}{4}\Delta^2 + [C^{(n)}\delta p_n]^2(1+\alpha^2)\right\}^{1/2}. \qquad (13)$$

Here $\mathbf{n}$ is the unit normal to the M-plane, the point $\mathbf{p}_M$ lies on the M-plane, $\delta p_n = \mathbf{n}(\mathbf{p} - \mathbf{p}_M)$, $C^{(n)} = C^{(n)}(\mathbf{p}_M)$ is the nth component of vector $\mathbf{C}$ at the point $\mathbf{p}_M$, $\alpha = D^{(n)}(\mathbf{p}_M)/C^{(n)}$, and $\Delta = \Delta(\mathbf{p}_M)$. Note that now the functions $\varepsilon_{m\rho}(\mathbf{p}_M)$ and $u_{m\mathbf{p}_M\rho}$ are smooth functions of $\mathbf{p}_M$ (their characteristic range of variation on the M-plane is $\sim G$). Figure 1a shows a typical constant-energy surface $\varepsilon_{m\rho}(\mathbf{p}) = E$ near the M-plane.

2) The vectors $\mathbf{B}$, $\mathbf{C}$, $\mathbf{D}$ are coplanar, with two possibilities.

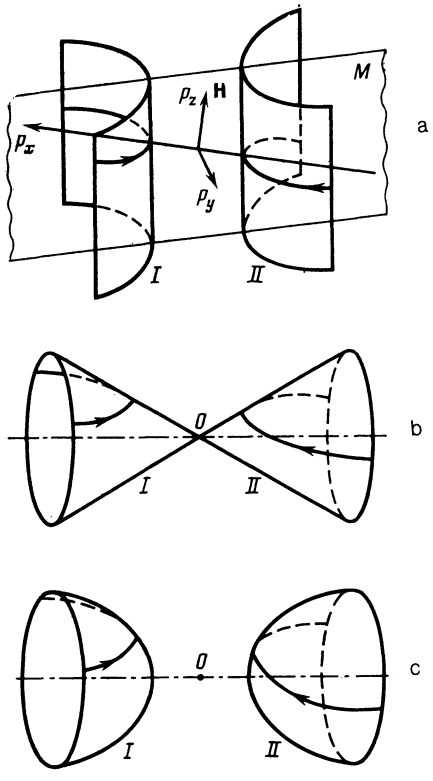

FIG. 1. Schematic diagram of portions of the constant-energy surfaces in regions of anomalous approach of two bands (I and II). Arrows indicate the direction of motion of conduction electrons along the trajectories (1). For clarity, spin splitting is not shown. a) M-plane spectrum. For simplicity, H lies in the M-plane. b) $\mathbf{p}_0$-curve spectrum (O is a point of unavoidable degeneracy). c) $\mathbf{p}_\Delta$-curve spectrum (O is the point of minimum band gap).

2a) $\mathbf{C} \| \mathbf{D}$, but $\mathbf{C}$ is not parallel to $\mathbf{B}$. $\Delta(\mathbf{p})$ vanishes along the intersection of the two planes

$$\mathbf{C}(\mathbf{p}')\delta\mathbf{p} = 0, \quad \mathbf{B}(\mathbf{p}')\delta\mathbf{p} = -\Delta(\mathbf{p}'). \qquad (14)$$

If the constant-energy surface $\varepsilon_{m\rho}(\mathbf{p}) = E$ intersects such a line of unavoidable degeneracy[5] ($\mathbf{p}_0$-line[4]), then the part of the surface near the line takes the form of an elliptic cone (see Fig. 1b). The interior regions corresponding to the different bands are separated by the point $\mathbf{p}_0 = \mathbf{p}_0(E)$, at which $\varepsilon_1(\mathbf{p}_0) = \varepsilon_2(\mathbf{p}_0) = E$. The procedure for choosing the functions $\varepsilon_{m\rho}(\mathbf{p})$ (and corresponding Bloch factors) with their analyticity taken into account, the equations describing the spectrum near the $\mathbf{p}_0$-line, and the equation of the elliptic cone, as presented in Ref. 4, may be easily generalized to the case at hand:

$$\varepsilon_{1\rho,2\rho}(\mathbf{p}) = \varepsilon(\mathbf{p}_0) + \frac{1}{2}\sum_{k=1}^{3}\delta p_k \operatorname{Sp}\hat{V}_k \pm \frac{1}{2}\Bigg[\Delta^2$$
$$+ \sum_{k,l=1}^{3}\{2\operatorname{Sp}(\hat{V}_l\hat{V}_k) - \operatorname{Sp}\hat{V}_l \operatorname{Sp}\hat{V}_k\}\delta p_l \delta p_k\Bigg]^{1/2}, \qquad (15)$$

$$A_1\delta p_1^2 + A_2\delta p_2^2 + A_3\delta p_3^2 = \Delta^2, \quad \delta\mathbf{p} = \mathbf{p} - \mathbf{p}_0, \quad \hat{V}_k = \hat{V}_k(\mathbf{p}_0). \qquad (15a)$$

Here $\Delta = \Delta(\mathbf{p}_0) \equiv 0$, while Eq. (15a) has been written out in a coordinate system in which the tensor $A_{lk} = \operatorname{Sp}\hat{V}_l \operatorname{Sp}\hat{V}_k - \operatorname{Sp}(\hat{V}_l, \hat{V}_k)$ is diagonal; the A_k are the

eigenvalues of the tensor A_{lk}, and the 3-axis is directed along the axis of the cone. In contrast to Ref. 4, taking the trace here also involves a summation over "spin" variables. In the present instance, this leads to the same renormalization factor $1+\alpha^2$ as in case (1).

2b) **C** is not parallel to **D**. Here it is essential that $\mathbf{D}\neq 0$, and naturally this has no analog in Ref. 4. As in case (1), the gap near $\mathbf{p}'$ is $\Delta(\mathbf{p})\neq 0$, but the minimum of $\Delta(\mathbf{p})$ occurs on the curve of anomalous approach (which we call the $\mathbf{p}_\Delta$-curve). The constant-energy surface near the $\mathbf{p}_\Delta$-curve may be approximated by a hyperboloid of two sheets, with $\mathbf{p}_\Delta=\mathbf{p}_\Delta(E)$. Equations (15) and (15a) are also valid here, but with

$$\Delta=\Delta(\mathbf{p}_\Delta)\neq 0, \quad \dot{V}_k=V_k(p_\Delta), \quad \delta\mathbf{p}=\mathbf{p}-\mathbf{p}_\Delta,$$

$$\varepsilon(\mathbf{p}_0)\to\frac{1}{2}\sum_m{}' \varepsilon_m(\mathbf{p}_\Delta).$$

The form of the constant-energy surface is shown in Fig. 1c.

3) The vectors **B**, **C**, **D** are linearly independent. Then $\min\Delta(\mathbf{p})=0$ occurs at an isolated point on the intersection of the line (14) and the plane $\mathbf{D}\cdot\delta\mathbf{p}=0$. If that point $\mathbf{p}_T$ happens to be on the surface $\varepsilon_{m\rho}(\mathbf{p})=E$, where $E=E_{\rm cr}$ is a critical value of the energy, then it becomes the vertex of a cone, and the spectrum is the same as in case (2a). In general, depending on the value of E, one obtains a spectrum with a necked-off discontinuity,[5] i.e., the spectrum near $\mathbf{p}_T$ for $E\neq E_{\rm cr}$ is well approximated either by a hyperboloid of two sheets [which reduces to case (2b)], or a hyperboloid of one sheet (the situation prior to necking off [5]). In the latter case, the band-overlap condition (1a) no longer holds, and there is only one band. This leads to intraband breakdown[5,17] in a magnetic field, which makes no contribution to the macroscopic characteristics of a metal (see Refs. 3, 4) and will not be considered further in the present paper.

To conclude this discussion of possible types of spectra having a small band gap, we wish to emphasize that the situation analyzed in (3) above depends markedly on the magnitude of E (the location of the chemical potential for the given metal), with three topologically different cases for the E-dependence. Thus, one obtains a combined electronic and topological transition of the Lifshitz type[3] with a so-called conical point, which makes this situation interesting for the study of magnetic breakdown of conduction electrons as a function of external pressure or changes in the concentration of an alloy. Note that in an application to MB, Nedorezov[19] has considered such an approach to studying the effects of a conical point on the magnetic susceptibility of a metal under Lifshitz transition conditions. We shall not investigate the E-dependence in the present paper, and for fixed E, case (3) reduces completely to the types of spectra considered under case (2) ($\mathbf{p}_0$- and $\mathbf{p}_\Delta$-curves).

Solutions of the system (10) for the matrix $\hat{R}(\mathbf{p}|\mathbf{p}')$ are derived in the Appendix.

3. We now consider CE motion in a magnetic field $\mathbf{H}=(0,0,H)$. In the quasiclassical approximation, these move along trajectories governed by (1), formed by the intersection of a constant-energy surface with a plane perpendicular to **H**. Conduction electrons with the same band index m and different spin indices ρ will in general follow slightly different trajectories, since when $H\neq 0$, Zeeman splitting of the "spin" levels takes place:

$$\Delta_z^{(m)}(\mathbf{p})=\varepsilon_{m\uparrow}(\mathbf{p})-\varepsilon_{m\downarrow}(\mathbf{p})=g^{(m)}(\mathbf{p})\,\mu_B H, \tag{16}$$

where $g^m(\mathbf{p})$ is the $\mathbf{p}$-dependent g-factor of the conduction electrons,[6,11,12] and μ_B is the Bohr magneton. Spin-orbit coupling gives rise to a difference between the CE g-factor and its value for a free electron. In the weak SOC approximation, we have [6,7]

$$|g(\mathbf{p})-g_0|/g_0\approx\xi/\Delta(\mathbf{p}).$$

As a rule, $\Delta_z\ll\xi\sim 10^{-3}$–$10^{-2}$ eV.

Far from regions of magnetic breakdown, we can neglect interband transitions and use results from the quasiclassical theory of metals.[5,18] To a first approximation in $\varkappa$, the quasiclassical wave function of a conduction electron in the $m\mathbf{P}$-representation takes the form (in this equation, we have used results from Ref. 18 and the appropriate expression from Ref. 4)

$$\Psi_{m\rho}(P_y)=\frac{c_{m\rho}}{|V_x^{(m)}|^{1/2}}\exp\left[\frac{ic}{e\hbar H}\left(P_x p_y-\int^{p_y}p_x(p_y')\,dp_y'\right)+i\gamma_{m\rho}{}^s\right]\chi_\rho\delta_{P_x P_{x0}}\delta_{p_z p_{z0}}\delta_{\rho\rho_0}, \tag{17}$$

where P_{x0}, p_{z0}, and ρ_0 are respectively the conserved projections of the generalized momentum ($\mathbf{P}=\mathbf{p}-(e/c)\mathbf{A}$) and "spin"; $\mathbf{A}=(Hy,0,0)$ is the vector potential; $V_x^{(m)}=\partial\varepsilon_m/\partial p_x$ is the x-component of velocity on the trajectory (1); $c_{m\rho}$ is an arbitrary constant factor;

$$p_x(p_y)=p_x^{(m)}(p_y,\ E,\ p_{z0}) \tag{17a}$$

is a solution of Eq. (1); and $\gamma_{m\rho}^s$ is the "spin" contribution to the phase of the quasiclassical function, which can be written in the form

$$\gamma_{m\rho}{}^s=\mp\frac{c\mu_B}{2e\hbar V_x^{(m)}}\int^{p_y}g^{(m)}(p_x(p_y'),p_y',p_{z0})\,dp_y'. \tag{18a}$$

The upper sign corresponds to $\rho=\uparrow$, and the lower to $\rho=\downarrow$. The integrals in Eqs. (17) and (18a) are evaluated along the classical trajectories (1), and χ_ρ is a "spin" function of the type (3): $\chi_\uparrow=\lambda\chi_\uparrow^0+\mu\chi_\downarrow^0$.

It is well known[6,12,19] that when a CE follows the trajectory (1), averaging of the g-factor takes place: the g-factor corresponding to an orbit with given E and p_{z0} is $g_c^{(m)}=g_c^{(m)}(p_{z0},E)$. Making the substitution $g\to g_c$ in (18a), we find after some straightforward manipulation

$$\gamma_{m\rho}{}^s=\pm(1/2\hbar)\,g_c^{(m)}\,\mu_B H t_{m\rho}, \tag{18b}$$

where $t_{m\rho}=t_{m\rho}(p_y,p_{z0},E)$ is the time along a trajectory with conserved m and ρ. In deriving (18b), we have used the classical equations of motion of a conduction electron[5]:

$$d\mathbf{p}/dt=(e/c)[\mathbf{VH}], \quad \mathbf{V}=\partial\varepsilon/\partial\mathbf{p}.$$

Note that Eq. (18b) is fully consistent with the result of Ref. 18.

When SOC is neglected far from MB regions [$\Delta(\mathbf{p})\approx\varepsilon_0$ outside these regions], $g_c\to g_0$ and $\chi_\rho\to\chi_\rho^0$ in (17) and (18b).

Within MB regions, the trajectories of conduction electrons approach one another rather closely ($p_{\min}\lesssim G\Delta/\varepsilon_0$), and $\Delta(\mathbf{p})\ll\varepsilon_0$. Note that for all of the spectral types considered [(13), (15), (15a) and Figs. 1a–1c], the classical tra-

jectories (1) with $\rho = \text{const}$ are, over the segment of closest approach, different branches of a single hyperbola (bearing in mind that ρ takes on two values, we obtain the situation depicted in Fig. 2). We also point out that the most interesting and frequently encountered situation is that of an M-plane (Fig. 1a) [see also the discussion preceding Eq. (13)]. In that case, a fairly thick sheet (in p_z) of trajectories is formed in the MB region, giving a siginificant probability of magnetic breakdown (see Ref. 4 and below). For the spectra depicted in Figs. 1b and 1c, we obtain narrow sheets of CE orbits that are effective for MB, since as the secant plane $p_z = \text{const}$ recedes from the symmetry axis, the probability of MB decreases, due to the rapid increase in $p_{\min}(p_z)$ (see Ref. 4 and below). The thickness of the narrow sheets, which depends on the magnetic field strength, is always less than the transverse size of the thick sheets, which is independent of the field strength for any reasonable field **H**.[3,4]

We next analyze M-plane spectra in more detail. For other spectral types, the change in the form of the s-matrix is discussed at the end of Sec. 3 [in conjunction with Eq. (31)].

When $H \neq 0$, it is necessary to construct an effective Hamiltonian in the MB region, which governs CE dynamics in the non-quasiclassical region (with characteristic size $\Delta P_y \ll G$; see Fig. 2), where interband transitions of conduction electrons are important. The method of constructing such a Hamiltonian formulated in Ref. 4 may be easily generalized to the case in which spin-orbit coupling is taken into account. One must then match the eigenfunctions of this Hamiltonian to the quasiclassical functions (17) and obtain the scattering matrix $\hat{s}$ relating the coefficients $c_{m\rho}$ on the two sides of the MB region (Fig. 2):

$$c_{m\rho}^{(+)} = \sum_{m'\rho'} s_{m\rho,m'\rho'} c_{m'\rho'}^{(-)}. \tag{19}$$

Without loss of generality, we assume here that the M-plane meets the plane $p_z = p_{z0}$ along the line $P_y = \bar{p}_y = 0$, and that the angle between **H** and the M-plane is θ. The plus and minus signs in (19) are chosen in accordance with the sign of $\delta P_y = p_y - \bar{p}_y = p_y$.

In the MB region, the square root in the dispersion relation (13) cannot be neglected, and the functions (17) are not applicable. As shown in Ref. 4, however, the smallness of $\varkappa$ and Δ/ε_0 make it possible to generalize the correspondence principle[3-5] to the case of magnetic breakdown. To do so, we must turn to the system of equations which governs the spectrum near the M-plane, which in the present case is obtained from (10) by replacing $\mathbf{p}'$ by $\mathbf{p}_M$, matrix elements with respect to $\mathbf{V}\cdot\delta\mathbf{p}$ by those with respect to $V^n \delta p_n$ and $R_{m\rho,m'\rho'}$ by $\beta_{m'\rho'}$. Here the $\beta_{m\rho}(\mathbf{p})$ are the expansion coefficients of the Bloch factors (3) in eigenfunctions of the Hamiltonian[3]

$$\hat{\mathcal{H}}(\mathbf{p}_M) = e^{-i\mathbf{p}_M\mathbf{r}/\hbar}\hat{\mathcal{H}}e^{i\mathbf{p}_M\mathbf{r}/\hbar}.$$

Note that the functions $\beta_{m\rho}(\mathbf{p})$ are in fact smooth functions of p_x, inasmuch as the p_x-axis lies in the M-plane.

According to the correspondence principle, we obtain the Schroedinger equation for $H \neq 0$, up to terms of order $\varkappa$, by making the substitution $\mathbf{p} \to \mathbf{P} + (e/c)\mathbf{A}$ in this system. The equations thus obtained govern the motion of a conduction electron in a magnetic breakdown region for constant magnetic field **H**. We can immediately extract from $\beta_{m\rho}(\mathbf{p})$ a rapidly varying exponential factor, leaving the smoothly varying amplitudes $\varphi_{m\rho}(p_y)$:

$$\beta_{m\rho}(\mathbf{P}) = \varphi_{m\rho}(p_y)\exp\left[i(c/e\hbar H)(P_{x0}-\bar{p}_x)p_y\right]\delta_{P_{x0}P_x}\delta_{p_{z0}p_z},$$
$$\frac{1}{2}\sum_m \varepsilon_m(\bar{p}_x, 0, p_{z0}) = E, \tag{20}$$

where $\bar{p}_x$ is determined by the second equality in (20). We have also made use of the assertion, which is proved in Ref. 4, that the two branches of Eq. (1) are independent.

Thus, in an MB region, the Schroedinger equation reduces to a system of four first-order differential equations (two in Ref. 4) for the $\varphi_{m\rho}(p_y)$:

$$iV_x\frac{e\hbar H}{c}\frac{\partial\varphi_{1\uparrow}}{\partial p_y} + \left(\bar{V}_y p_y + \frac{\bar{\Delta}}{2} + \frac{\bar{\Delta}_z^{(1)}}{2}\right)\varphi_{1\uparrow}$$
$$+\bar{C}_y p_y \varphi_{2\uparrow} + \bar{D}_y p_y \varphi_{2\downarrow} = 0,$$
$$iV_x\frac{e\hbar H}{c}\frac{\partial\varphi_{1\downarrow}}{\partial p_y} + \left(\bar{V}_y p_y + \frac{\bar{\Delta}}{2} - \frac{\bar{\Delta}_z^{(1)}}{2}\right)\varphi_{1\downarrow}$$
$$\pm\bar{C}_y p_y \varphi_{2\downarrow} \mp \bar{D}_y p_y \varphi_{2\uparrow} = 0,$$
$$iV_x\frac{e\hbar H}{c}\frac{\partial\varphi_{2\uparrow}}{\partial p_y} + \left(\bar{V}_y p_y - \frac{\bar{\Delta}}{2} + \frac{\bar{\Delta}_z^{(2)}}{2}\right)\varphi_{2\uparrow}$$
$$+\bar{C}_y p_y \varphi_{1\uparrow} \mp \bar{D}_y p_y \varphi_{1\downarrow} = 0,$$
$$iV_x\frac{e\hbar H}{c}\frac{\partial\varphi_{2\downarrow}}{\partial p_y} + \left(\bar{V}_y p_y - \frac{\bar{\Delta}}{2} - \frac{\bar{\Delta}_z^{(2)}}{2}\right)\varphi_{2\downarrow}$$
$$\pm\bar{C}_y p_y \varphi_{1\downarrow} + \bar{D}_y p_y \varphi_{1\uparrow} = 0, \tag{21}$$

where

$$\bar{\Delta} = \varepsilon_1(\bar{\mathbf{p}}) - \varepsilon_2(\bar{\mathbf{p}}),\quad \bar{\mathbf{p}} = (\bar{p}_x, 0, p_{z0}),\quad \bar{C}_y = C_y(\bar{\mathbf{p}}),$$
$$\bar{D}_y = D_y(\bar{\mathbf{p}}),\quad V_x = \partial\varepsilon_M/\partial\bar{p}_x,$$
$$\varepsilon_M = [\varepsilon_1(\bar{\mathbf{p}}) + \varepsilon_2(\bar{\mathbf{p}})]/2,\quad \bar{V}_y = V_{m,m}^{(y)}(\bar{p})\cos\theta,$$
$$\bar{\Delta}_z^{(m)} = g^{(m)}(\bar{\mathbf{p}})\mu_B H.$$

The plus and minus signs are chosen in accordance with (11).

As our estimates indicate, $\bar{\Delta}_z^{(m)}$ remains much smaller than $\bar{\Delta}$ even for fields $H \sim H_0 = \bar{\Delta}^2/4\mu_B\varepsilon_0$, in which the probability of MB is of order unity[2-4]

$$\bar{\Delta}_z^{(m)} = g^{(m)}\mu_B H_0 \approx g^{(m)}\bar{\Delta}^2/4\varepsilon_0 \ll \bar{\Delta}.$$

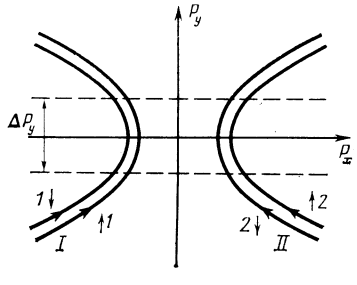

FIG. 2. Schematic diagram of segments of quasiclassical trajectories (1) near a magnetic breakdown region. The band index m and spin direction are given next to the arrows indicating the direction of CE motion.

The g-factor should then be much less than 10^3–10^4, which is true even for the "needle" electrons in Zn [$g^n \sim 100$ (Ref. 15)]. In the following calculations, we neglect $\bar{\Delta}_z^{(m)}$.

Let us introduce the new functions $F_i(x)$ $(i = 1,2,3,4)$:

$$F_{1,3}[x(p_y)] = \exp[-i(c/e\hbar H)p_y^2 \bar{V}_y/2V_x](\varphi_{1\uparrow} \pm \varphi_{2\uparrow}); \quad (22)$$

$F_{2,4}$ are obtained by replacing $\uparrow$ by $\downarrow$ in (22); $x = (c/e\hbar H)^{1/2} p_y |\bar{C}_y/V_x|^{1/2}$. Omitting the lower signs in (21) (the results are the same in either case), we obtain the following set of equations:

$$idF_1/dx + aF_3 + xF_1 - \bar{\alpha} x F_4 = 0, \quad (23a)$$

$$idF_3/dx + aF_1 - xF_3 + \bar{\alpha} x F_2 = 0, \quad (23b)$$

$$idF_2/dx + aF_4 + xF_2 + \bar{\alpha} x F_3 = 0, \quad (23c)$$

$$idF_4/dx + aF_2 - xF_4 - \bar{\alpha} x F_1 = 0, \quad (23d)$$

where

$$a = (\bar{\Delta}/2)(c/e\hbar H)^{1/2} |V_x \bar{C}_y|^{-1/2}, \quad \bar{\alpha} = \bar{D}_y/\bar{C}_y.$$

Notice that when $\bar{\alpha} = 0$, the equations in (23) separate into two independent systems for the two Ce spin directions. These systems of two equations are similar to Eqs. (A2) of Ref. 4, but are not identical.[2)]

Eliminating F_3 from (23a) and (23b), and F_2 from (23c) and (23d), we obtain

$$d^2F_1/dx^2 + [a^2 + x^2(1+\bar{\alpha}^2) - i]F_1 + i\bar{\alpha}F_4 = 0, \quad (24a)$$

$$d^2F_4/dx^2 + [a^2 + x^2(1+\bar{\alpha}^2) + i]F_4 + i\bar{\alpha}F_1 = 0. \quad (24b)$$

Eliminating F_4, we can then represent the resulting fourth-order differential equation in the form

$$\hat{O}_\nu \Phi(\nu) = 0, \quad (25a)$$

where

$$\Phi(\nu) = \hat{O}_\nu^* F_1(\nu), \quad (25b)$$

$\nu = \beta x$, $\beta = (1 + \bar{\alpha}^2)^{1/2}$, and the differential operator

$$\hat{O}_\nu = d^2/d\nu^2 + [a^2/\beta + \nu^2 + i],$$

the choice of sign preceding the i being irrelevant.

The general equation (25a) is a superposition of parabolic cylinder functions $D_\lambda(\nu)$:

$$F_1(\nu) = k_1 y_1(\nu) + k_2 y_2(\nu) + k_3 y_3(\nu) + k_4 y_4(\nu), \quad (26a)$$

where the k_i are arbitrary constants;

$$y_{1,2} = \mathcal{D}_{-ia^2/2\beta - 1}[\pm(1+i)\nu], \quad y_{3,4} = \mathcal{D}_{-ia^2/2\beta}[\pm(1+i)\nu],$$

$y_{1,2}$ is the solution of the homogeneous equation corresponding to (25b), and $y_{3,4}$ is the solution of Eq. (25a) (Ref. 20).[3)] We find the other F_i from (23) and (24), taking advantage of the properties of the parabolic cylinder functions[20]:

$$F_2 = \frac{\beta^{1/2}}{a}\left[(1-i)\left(\frac{\beta-1}{\beta+1}\right)^{1/2}(k_1 y_3 - k_2 y_4) + \frac{a^2}{2\beta}(1+i)\left(\frac{\beta+1}{\beta-1}\right)^{1/2}(-k_3 y_1 + k_4 y_2)\right], \quad (26b)$$

$$F_3 = \frac{\beta^{1/2}}{a}\left[(1-i)(-k_1 y_3 + k_2 y_4) + \frac{a^2}{2\beta}(1+i)(-k_3 y_1 + k_4 y_2)\right], \quad (26c)$$

$$F_4 = -\left(\frac{\beta-1}{\beta+1}\right)^{1/2}(k_1 y_1 + k_2 y_2) + \left(\frac{\beta+1}{\beta-1}\right)^{1/2}(k_3 y_3 + k_4 y_4). \quad (26d)$$

In matching the functions (17) and (26), we make use of the following propositions, generalized to the SOC case, which are proved in Ref. 4 for the "spinless" problem.

The region of applicability of the quasiclassical expressions (17), $|\delta P_y| \gg (e\hbar H/c)^{1/2}$, and the region in which the quantum equations (21) are valid, $|\delta P_y| \ll G$, overlap. Within the overlap region, $\Psi_{m\rho}$ and $\beta_{m\rho}$ may be related via the unitary matrix $\hat{R}$ to order $\varkappa$:

$$\beta_{m\rho}(P_y) = \sum_{m'\rho'} R_{m'\rho',m\rho}(p_x^{(m\rho)}(P_y), P_y, p_{z0} | \bar{p}_x, 0, p_{z0}) \Psi_{m'\rho'}^{(\pm)}(P_y). \quad (27)$$

The plus or minus sign depends on the sign of P_y, and the behavior of $p_x^{(m\rho)}(P_y)$ in $R_{m\rho,m'\rho'}$ and $\Psi_{m\rho}$ is determined by Eq. (17a). Note that in the interval in question, we can disregard, to the indicated accuracy, the contribution from CE spin both to the phase of $\Psi_{m\rho}$, i.e., we can put $\gamma_{m\rho}^s = 0$ in (17), and to $R_{m'\rho',m\rho}$: $p_x^{(m\rho)}(P_y) \to p_x^{(m)}(P_y)$.

Over the indicated range, in the chosen coordinate system,

$$\hat{R} = \begin{pmatrix} 2^{-1/2} & 0 & 2^{-1/2}\beta^{-1}\operatorname{sign} P_y & 2^{-1/2}\bar{\alpha}\beta^{-1}\operatorname{sign} P_y \\ 0 & 2^{-1/2} & \mp 2^{-1/2}\bar{\alpha}\beta^{-1}\operatorname{sign} P_y & \pm 2^{-1/2}\beta^{-1}\operatorname{sign} P_y \\ -2^{-1/2}\beta^{-1}\operatorname{sign} P_y & \pm 2^{-1/2}\bar{\alpha}\beta^{-1}\operatorname{sign} P_y & 2^{-1/2} & 0 \\ -2^{-1/2}\bar{\alpha}\beta^{-1}\operatorname{sign} P_y & \mp 2^{-1/2}\beta^{-1}\operatorname{sign} P_y & 0 & 2^{-1/2} \end{pmatrix}, \quad (28)$$

where the choice of signs corresponds to (11) (see the Appendix as well).

Employing this matrix $\hat{R}$, the asymptotic form of the functions $F_i(x)$ as $x \to -\infty$ (Ref. 20), and Eqs. (13), (17), (17a), (20), (22), and (26), we can use Eq. (27) to express the coefficients k_i in terms of the $c_{m\rho}^{(-)}$. The asymptotic behavior of the F_i for $x \to +\infty$ (Ref. 20) and the same equations give the relationship between the $c_{m\rho}^{(+)}$ and k_i. Eliminating the k_i, we obtain in final form the unitary fourth-rank s-matrix with no restrictions on the magnitude of $\bar{\alpha}$:

$$\hat{s} = \begin{pmatrix} \tau e^{-i\Lambda} & 0 & \sigma/\beta & \pm\bar{\alpha}\sigma/\beta \\ 0 & \tau e^{-i\Lambda} & \mp\bar{\alpha}\sigma/\beta & \sigma/\beta \\ -\sigma/\beta & \pm\bar{\alpha}\sigma/\beta & \tau e^{i\Lambda} & 0 \\ \mp\bar{\alpha}\sigma/\beta & -\sigma/\beta & 0 & \tau e^{i\Lambda} \end{pmatrix}, \quad (29)$$

where

$$\Lambda = \left[\frac{\pi}{4} + \frac{H_0}{\pi H} + \arg\Gamma\left(i\frac{H_0}{\pi H}\right) - \frac{H_0}{\pi H}\ln\frac{H_0}{\pi H}\right]\operatorname{sign}[\varepsilon_1(\bar{\mathbf{p}}) - \varepsilon_2(\bar{\mathbf{p}})],$$

$$H_0 = \frac{c\pi\bar{\Delta}^2}{4e\hbar\beta |V_x V_{\uparrow\uparrow,2\uparrow}^{(n)} \cos\theta|}, \quad \sigma = e^{-H_0/2H}, \quad \sigma^2 + \tau^2 = 1, \quad (29a)$$

and $\Gamma(x)$ is the gamma function.[20] Notice that all elements in (29) and (29a) are expressed in terms of the CE dispersion relation for $H = 0$ in the M-plane.

Thus, taking spin-orbit coupling into consideration leads to a probability of MB with spin flip

$$w_{\uparrow\downarrow}=w_{\downarrow\uparrow}=|s_{1\uparrow,2\downarrow}|^2=[\bar{\alpha}^2/(1+\bar{\alpha}^2)]e^{-H_0/H}, \qquad (30)$$

which shows the exponential dependence on the reciprocal of the magnetic field characteristic of MB theory.[2,3] It is interesting to note that the probability for a CE to remain in its own band, $\tau^2 = 1 - \exp(-H_0/H)$, appears formally the same as in Ref. 4. But the field H_0 has itself been renormalized: taking SOC into account reduces H_0 compared to its former value H_0^0 at $\bar{\alpha} = 0$ (see the second footnote):

$$H_0=H_0^0(1+\bar{\alpha}^2)^{-1/2}.$$

Spin-orbit coupling therefore results in a reduction in the field strength H at which MB becomes important, or from another point of view, since $\bar{\Delta}$ is usually determined from MB experiments,[2,3,15,21] SOC makes MB possible in metals with a larger band gap Δ than would otherwise be the case.

It is easily seen from (29) that for $\bar{\alpha} = 0$ (no SOC), the matrix (29) separates into two independent second-rank matrices for both CE spin directions. By virtue of the minor correction (see the second footnote), both of these matrices are the same as those determined in Ref. 4.

Note that for the spectra diagrammed in Figs. 1b and 1c, the s-matrix (29) retains the same form, and only the form of H_0 changes. For the spectrum with a degenerate point (Fig. 1b), SOC results in the same renormalization known from Refs. 3 and 4 for H_0^0 [Eq. (3.2.13) of Ref. 3]:

$$H_0(E, p_z)=A(E, \eta)(c/e\hbar\beta)[p_z-(p_0)_z(E, \eta)]^2, \qquad (31)$$

where $\eta = \mathbf{H}/H$; $(p_0)_z$ is the z-component of the conical degenerate point of the constant-energy surface with energy E; $A(E,\eta)$ is a dimensionless quantity of order unity, which depends essentially on the geometry of the cone [the parameters A_k in (15a)] and η (the explicit form of A is given in Ref. 4).

For the spectrum shown in Fig. 1c, a term of order $\Delta^2/e\hbar\beta V_0$ is added to the right-hand side of Eq. (31), and $\mathbf{p}_0 \to \mathbf{p}_\Delta$.

4. We now investigate the CE spectrum under coherent breakdown conditions. The small size of the MB regions [these are of order $(\Delta/\varepsilon_0)G$ for a breakdown probability of order unity] enables us to treat them as points, and we refer to them as MB vertices.[3,9] Figure 3 shows a schematic diagram of an MB vertex (compare this with Fig. 2). There is a non-zero probability for a conduction electron moving along any quasiclassical trajectory toward an MB vertex to be found after breakdown on three of the four segments of quasiclassical trajectories leaving the MB vertex, including those having a different band index and spin direction. Such "scattering" occurs in accordance with the structure of the s-matrix (29).

The quasiclassical segments associated with MB vertices form an MB configuration which can be quite complicated.[3] We are dealing with twice as many segments as in Ref. 3, since two of the previous MB configurations with different spins are combined into one, given that $w_{\uparrow\downarrow} \neq 0$.

Since the wave-function phase accumulated by conduction electrons over identical parts of the MB configuration is

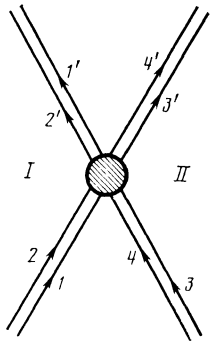

FIG. 3. An MB vertex (1–4 are incoming segments of quasiclassical trajectories, 1'–4' are outgoing).

the same, multiple scattering from MB vertices produces an interference pattern, giving rise to a unique MB spectrum for the conduction electrons. This is known as coherent magnetic breakdown,[3] in which collisions fail to disrupt the MB spectrum ($\omega_c \gg \omega$, where $\omega = \max\{\omega_{\text{imp}}, \omega_{\text{sa}}\}$; ω_{imp} is the rate of electron-impurity scattering, and ω_{sa} is the rate of small-angle scattering).

Note that for $\omega_{\text{sa}} \gg \omega_c \gg \omega_{\text{imp}}$ collisions destroy this coherence, the MB spectrum is disrupted (conduction electrons jump randomly from orbit to orbit), and stochastic MB ensues.[3]

The mathematical tools developed in Ref. 3 to analyze MB configurations and construct dispersion relations do not constrain the form of the s-matrix or its rank. We therefore first present certain equations which generalize the results obtained in that paper. Following the same terminology, we assign different indices i, j to inequivalent segments with quasiclassical motion. In general, CE motion in an MB configuration is described by a stationary wave function

$$\Psi=\sum_{i=1}^{N} c_i\Psi_i(P_y)\delta_{P_{x_0}P_x}\delta_{P_{z_0}P_z}, \qquad (32)$$

which is a superposition of quasiclassical wave functions Ψ_i for different segments; $\{m\rho\} = \{m\rho\}(i)$; and N is the number of segments in a closed MB configuration (for an open MB configuration, N is the number of inequivalent segments). The dependence of the MB vertices on the elements of the s-matrix is contained in the amplitudes c_i, which satisfy the system of linear equations

$$c_i-\sum_{j=1}^{N} V_{ij}^{(0)}e^{i\tilde{\gamma}_j}c_j=0,$$

$$\tilde{\gamma}_j(E, p_z)=\gamma_j+Rn_j+(\Lambda_{\bar{j}}+\Lambda_j)/2. \qquad (33)$$

Here $\gamma_j(E, p_z) = S_j/\hbar + \gamma_j^s + \delta_j$ is the classical phase of the wave function (17) accumulated over the jth segment between two successive MB scatterings; $S_j(E, p_z)$ is the increment in the transverse action

$$\frac{c}{eH}\int_{p_{y_j}}^{p_{y_j}} p_x^{(j)}dp_{y_j}$$

with spin not taken into account; γ_j^s is the spin contribution to the phase of (17); in Eq. (18), we must make the replacement $t_{m\rho}(E, p_z) \to T_j(E, p_z)$; $\delta_j = \pm\pi/2$ is the sum of all phase jumps occurring over the jth segment at the classical turning points[3,9,18] (note that γ_j^s was not taken into consi-

deration in Ref. 3); $\bar{j}$ is the number of the segment entering the MB vertex from which segment j emerges, with $m(j) = m(\bar{j})$; $R = cG_y P_x / e\hbar H$; $n_j = 0$ for closed MB configurations; $n_j = 0$ for open MB configurations if j is an interior segment, and $n_j = \operatorname{sign}(\partial P_y / \partial P_x)$ for segments which cross the boundary of an elementary cell[3]; $\hat{V}^0$ is a unitary matrix of rank N, in which only three elements per column (two in Ref. 31) are non-zero:

$$V^{(0)}_{i,j} = s^{(0)}_{m'\rho',m\rho}, \quad i = i(m',\rho'), \quad j = j(m,\rho),$$

and these elements occur in rows with the same indices as those of the segments connected to segment j by a common MB vertex; $\hat{s}^{(0)}$ is the s-matrix, in which all $\Lambda = 0$.

The condition for the system (33) to be solvable leads to the dispersion relation

$$D(\tilde{\gamma}) = \det[\hat{I} - \hat{U}^{(0)}(\{\tilde{\gamma}_i\})] = 0, \quad U^{(0)}_{ij} = V^{(0)}_{ij} e^{i\tilde{\gamma}_j}. \quad (34)$$

In general, $D(\tilde{\gamma})$ is a finite trigonometric polynomial in $\tilde{\gamma}_i$, whose coefficients depend solely on the MB probabilities (σ^2, τ^2, and $\bar{\alpha}^2$).

The MB spectrum is determined from the solution of the transcendental equation (34); for a closed MB configuration, we have a discrete set of Landau levels, modified by MB, and for an open MB configuration, we have a set of magnetic bands.

We now apply the foregoing procedure to the analysis of a simple MB configuration (Fig. 4). In the limiting case of no SOC ($\bar{\alpha} = 0$), this degenerates into two independent figure-eights, which were analyzed in Ref. 3 (Fig. 4a in Ref. 3). For our double figure-eight we have $i = 1$–4, with 1, 2 corresponding to CE motion in the first band, 3, 4 to motion in the second band, odd parity being spin up (↑), even parity being spin down (↓), and $n_i = 0$. The dispersion equation (34) reduces to the form

$$\begin{aligned} D(\gamma) = {} & \cos\left(\frac{\Sigma\gamma_i}{2}\right) - \tau\left(\cos\frac{\gamma_1+\gamma_2+\gamma_3-\gamma_4}{2} + \cos\frac{\gamma_1+\gamma_2-\gamma_3+\gamma_4}{2}\right. \\ & \left. + \cos\frac{\gamma_1-\gamma_2+\gamma_3+\gamma_4}{2} + \cos\frac{-\gamma_1+\gamma_2+\gamma_3+\gamma_4}{2}\right) \\ & + \tau^2\left(\cos\frac{\gamma_1+\gamma_2-\gamma_3-\gamma_4}{2}\right. \\ & \left. + \cos\frac{\gamma_1-\gamma_2+\gamma_3-\gamma_4}{2} + \cos\frac{-\gamma_1+\gamma_2+\gamma_3-\gamma_4}{2}\right) + \frac{\sigma^2}{1+\bar{\alpha}^2} \\ & \cdot\left(\cos\frac{\gamma_1-\gamma_2+\gamma_3-\gamma_4}{2} + \bar{\alpha}^2\cos\frac{\gamma_1-\gamma_2-\gamma_3+\gamma_4}{2}\right) = 0. \end{aligned} \quad (35)$$

In the limit $\bar{\alpha} = 0$, Eq. (35) can be factored:

$$\begin{aligned} D^0(\gamma) = {} & \left(\cos\frac{\gamma_1+\gamma_3}{2} - \tau\cos\frac{\gamma_1-\gamma_3}{2}\right) \\ & \times\left(\cos\frac{\gamma_2+\gamma_4}{2} - \tau\cos\frac{\gamma_2-\gamma_4}{2}\right). \end{aligned} \quad (35a)$$

If we assume that $\gamma_i^s = 0$ here, then every factor in (35a) is identical with the function D for a simple figure-eight [Eq. (3.2.30) in Ref. 3].

We wish to emphasize an important property of MB: there exist two quasiclassical limits (depending on the magnitude of H), with $\sigma^2\tau^2 = 0$.

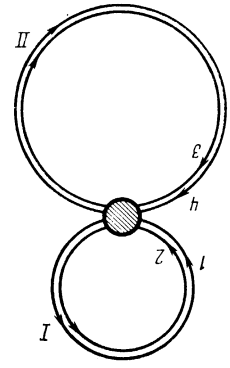

FIG. 4. Closed MB configuration (i = 1–4 is the segment index).

1) $\sigma = 0$, $\tau = 1$ ($H \ll H_0$): no magnetic breakdown. Conduction electrons move in orbits with no change in i, and Eq. (35) can be factored as

$$D_{\sigma=0}(\gamma) = 8\sin(\gamma_1/2)\sin(\gamma_2/2)\sin(\gamma_3/2)\sin(\gamma_4/2). \quad (36)$$

It is easy to obtain from (36) the usual Lifshitz-Onsager quantization conditions with spin splitting taken into account,[5,18] and for each of the quasiclassical trajectories,

$$\tilde{S}_i \pm \pi\mu_B H g_i m_c^{(i)} = \frac{2\pi e\hbar H}{c}\left(n + \frac{1}{2}\right), \quad n = 0, 1, 2, \ldots \quad (36a)$$

where $\tilde{S}_i(E, p_z)$ is the cross-sectional area of the constant-energy surface in the m-band ($m = m(i)$, $\tilde{S}_1 = \tilde{S}_3$, $\tilde{S}_2 = \tilde{S}_4$); $m_c^{(i)} = eHT_i/2\pi c = (\partial\tilde{S}/\partial E)_i/2\pi$ is the cyclotron mass of a conduction electron on segment i ($m_c^1 = m_c^2$, $m_c^3 = m_c^4$); g_i is the CE g-factor on segment i ($g_1 = g_2 = g_c^{(1)}(E, p_z)$, $g_3 = g_4 = g_c^{(2)}(E, p_z)$). The definition (16) of the g-factor is consistent with that in Refs. 6–8, 11, 12, 19, and 22–24, but it differs from $\tilde{g}$ in Refs. 5 and 18. The relationship between them is $\tilde{g} = gm_c/m$.

2) $\sigma = 1$, $\tau = 0$ ($H \gg H_0$): total breakdown. Almost all conduction electrons on the constant-energy surface move without "noticing" band gaps. The main difference between this and Ref. 3 is the possibility, due to the fact that $\bar{\alpha} = 0$, of a CE spin flip for every "encounter" with an MB vertex (30):

$$\begin{aligned} D_{\sigma=1}(\gamma) = {} & \cos\left(\frac{\Sigma\gamma_i}{2}\right) + \frac{1}{1+\bar{\alpha}^2}\left(\cos\frac{\gamma_1-\gamma_2+\gamma_3-\gamma_4}{2}\right. \\ & \left. + \bar{\alpha}^2\cos\frac{\gamma_1-\gamma_2-\gamma_3+\gamma_4}{2}\right). \end{aligned} \quad (37)$$

By analogy with (36a), making use of (37), we can write out the modified Lifshitz-Onsager magnetic breakdown condition for new orbits:

$$\tilde{S}_\sigma \pm \pi\mu_B H g_\sigma m_c^\sigma = \frac{2\pi e\hbar H}{c}\left(n + \frac{1}{2}\right), \quad (37a)$$

where $m_c^{(\sigma)} = m_c^1 + m_c^3$; $\tilde{S}_\sigma = \tilde{S}_1 + \tilde{S}_3$ is the total area of the figure-eight (Fig. 4), disregarding spin splitting; and the g-factor of the new orbit

$$\begin{aligned} g_\sigma(E, p_z) = {} & \frac{2m}{\pi m_c^\sigma}\arccos\left\{\frac{1}{1+\bar{\alpha}^2}\cos\left[\frac{\pi}{2m}(g_1 m_c^{(1)}\right.\right. \\ & \left.\left. + g_3 m_c^{(3)})\right] + \frac{\bar{\alpha}^2}{1+\bar{\alpha}^2}\cos\left[\frac{\pi}{2m}(g_1 m_c^{(1)} - g_3 m_c^{(3)})\right]\right\} \end{aligned} \quad (38)$$

is expressed in terms of the characteristics (g_i, m_c^i) of the segments and the SOC parameter $\overline{\alpha}$.

Notice that we obtain new information even when $\overline{\alpha}=0$, namely a formula for g_{av}, the g-factor averaged over the new orbits:

$$g_{av}=g_\sigma^{\,0}=(g_1 m_c^{(1)}+g_3 m_c^{(3)})/m_c^{(\sigma)}. \tag{38a}$$

It was pointed out in Refs. 3, 4, and 9 that in an intermediate case of well-developed MB ($\sigma^2\tau^2\neq 0$, $H\sim H_0$), the energy $E_n(E,p_z)$ becomes a quasirandom function of p_z. This is due to the fact that the phase $S_i/\hbar$ and its derivatives are in general incommensurate. We can obviously make the same statement about $g(E,p_z)$ when $\sigma^2\tau^2\neq 0$. Thus, the g-factors of an MB configuration will in general be spread over an interval

$$\min\{g(E,p_z)\}\leqslant g\leqslant\max\{g(E,p_z)\}. \tag{39}$$

This should lead, for example, to broadening of the CE paramagnetic resonance (CEPR) line under conditions of well-developed MB.[22-24]

5. To conclude, we can say that introducing spin-orbit coupling and a "spin" contribution to the phase of the quasiclassical function (17) leads to a number of interesting consequences. There is a nonvanishing probability of conduction electrons spin flip during MB [Eq. (30)]. Because of SOC, the MB field H_0 is reduced, making it possible to reappraise and augment existing data on band-gap sizes derived from MB experiments[2,3,15,21] in metals in which SOC significantly affects the CE spectrum (especially when Δ is essentially a spin-orbit gap).

Under stochastic MB conditions with CEPR, small MB regions emerge as additional scattering centers, broadening the CEPR lines from the hollows of the Fermi surface which are associated with MB.[22,23] Such broadening can also take place with coherent MB because of the wide spread in the g-factors of orbits with differing p_z which fall within an MB sheet (39). Thus, in Zn, MB associated with "needle" and "monster" conduction electrons broadens the CEPR monster lines,[22,23] with the result that the signal from the monster CE cannot be detected experimentally.[23] In Mg, another hexagonal metal, MB can account for the characteristic dependence on the direction of **H**: the line width from a monster CE is well described by[22]

$$\Delta H=\Delta H_{res}+\Delta H_{MB}\exp(-H_0^{(\theta=0)}/H\cos\theta),$$

where ΔH_{MB} is the CEPR "magnetic breakdown" line width, and ΔH_{res} is the residual line width. Estimates of ΔH_{res} and ΔH_{MB} (Ref. 22) are consistent with the results of CEPR experiments in Mg (Refs. 23, 24).

Interference between quasiclassical CE states of different spin during coherent MB should also show up, for example, in the de Haas-van Alphen effect.[3]

The author is sincerely grateful to M. I. Kaganov and B. I. Kochelaev for the formulation of this problem, and for their advice and unfailing attention, and to A. A. Slutskin for fruitful discussions.

APPENDIX

The spectrum (12) is doubly degenerate, with $\varepsilon_{m\uparrow}=\varepsilon_{m\downarrow}=\varepsilon_m$, which in general leads to a degree of arbitrariness in the determination of the fundamental system of equations (10) for $R_{m\rho,m'\rho'}(\mathbf{p}|\mathbf{p}')$. In order to eliminate this ambiguity, we require first that when $\mathbf{D}=0$, these solutions transform into the appropriate solutions of the analogous problem in Ref. 4, as described in the new augmented basis of wave functions incorporating CE spin (3), and secondly, that when $\delta\mathbf{p}\to 0$, the matrix $\hat{R}$ become diagonal, which follows from its definition (7). The latter equation also implies the unitarity of $\hat{R}$.

Substituting $E=\varepsilon_{1\rho}$ from (12) into (10), we obtain the following fundamental system of solutions to (10), which satisfies the foregoing conditions:

$$R_{1\uparrow,m'\rho'}=\left(R_0,0,-\frac{C\delta\mathbf{p}}{Y}R_0,-\frac{D\delta\mathbf{p}}{Y}R_0\right),$$

$$R_{1\downarrow,m'\rho'}=\left(0,R_0,\pm\frac{D\delta\mathbf{p}}{Y}R_0,\mp\frac{C\delta\mathbf{p}}{Y}R_0\right),$$

where

$$m'\rho'=1\uparrow,\ 1\downarrow,\ 2\uparrow,\ 2\downarrow,\quad R_0=[2Z/(X-\Delta X^{1/2})]^{1/2},\quad Y=2Z/(\Delta-X^{1/2}),$$
$$Z=(C\delta\mathbf{p})^2+(D\delta\mathbf{p})^2,\quad X=\Delta^2+4Z.$$

The choice of plus or minus signs corresponds to (11). From the system (10), it is straightforward to find $R_{2\rho,m'\rho'}(\mathbf{p}|\mathbf{p}')$ for $E=\varepsilon_{2\rho}$ from (12).

[1)] To make the estimates interpretable, we can represent the Bloch functions as orthogonal plane waves or associated plane waves[12,14]; $\xi^{(m)}$ is then replaced by the SOC energy for the corresponding atomic level in the metal comprising the crystal.[6]

[2)] The quantity a in Ref. 4 is twice as large, increasing H_0 (the MB field) by a factor of four. The corrected value of H_0 is consistent with other work in MB theory.[3,8,13]

[3)] The Wronskian is $W(\{y_i\})=2\pi[\Gamma(ia^2/2\beta)\Gamma(ia^2/2\beta+1)]^{-1}\neq 0$, as it should be for the basic set of equations.

[1] M. H. Cohen and L. M. Falicov, Phys. Rev. Lett. **7**, 231 (1961).
[2] R. W. Stark and L. M. Falicov, Progr. Low Temp. Phys. **5**, 735 (1967).
[3] M. I. Kaganov and A. A. Slutskin, *Elektrony provodimosti (Conduction Electrons)*, Nauka, Moscow (1985), p. 101.
[4] A. A. Slutskin, Zh. Eksp. Teor. Fiz. **53**, 767 (1967) [Sov. Phys. JETP **26**, 474 (1968)].
[5] I. M. Lifshitz, M. Ya. Azbel', and M. I. Kaganov, *Elektronnaya teoriya metallov (Electron Theory of Metals,* Consultant's Bureau, New York, 1973), Nauka, Moscow (1971).
[6] J. Jafet, Solid State Phys. **14**, 1 (1963).
[7] G. L. Bir and G. E. Pikus, *Simmetriya i deformatsionnye defekty v poluprovodnikakh,* Nauka, Moscow (1972) (*Symmetry and Strain-Induced Defects in Semiconductors,* Wiley, New York, 1975).
[8] E. I. Blount, Phys. Rev. **126**, 1636 (1962).
[9] A. A. Slutskin, Zh. Eksp. Teor. Fiz. **58**, 1098 (1970) [Sov. Phys. JETP **31**, 589 (1970)]; Zh. Eksp. Teor. Fiz. **65**, 2114 (1973) [Sov. Phys. JETP **38**, 1057 (1974)].
[10] M. I. Kaganov and Yu. N. Proshin, Fiz. Tverd. Tela (Leningrad) **28**, 1226 (1986) [Sov. Phys. Solid State **28**, 689 (1986)].
[11] V. F. Gantmakher and I. B. Levinson, *Rasseyanie nositelei toka v metallakh i poluprovodnikakh (Carrier Scattering in Metals and Semiconductors,* North-Holland, Amsterdam, 1987), Nauka, Moscow (1984); A. M. de Graaf and A. W. Overhauser, Phys. Rev. **180**, 701 (1969).
[12] F. Beuneu, J. Phys. F **10**, 2875 (1980).
[13] A. Pippard, *Fizika metallov, Dynamics of Conduction Electrons,* Gordon and Breach, New York (1965).
[14] A. P. Cracknell and K. C. Wong, *Fermi Surface: Its Concept, Determination, and Use in Physics of Metals,* Clarendon Press, Oxford (1973).
[15] J. P. van Dyke, J. W. McClure, and J. F. Doar, Phys. Rev. B **1**, 2551 (1970).
[16] A. A. Slutskin and A. M. Kadigrobov, Fiz. Tverd. Tela **9**, 184 (1967) [Sov. Phys.—Solid State **9**, 139 (1967)].
[17] G. E. Zil'berman, Zh. Eksp. Teor. Fiz. **32**, 296 (1957) [Sov. Phys. JETP **5**, 208 (1957)]; Zh. Eksp. Teor. Fiz. **33**, 386 (1957) [Sov. Phys. JETP **6**, 299 (1958)]; Zh. Eksp. Teor. Fiz. **34**, 515 (1958) [Sov. Phys. JETP **7**, 355 (1958)].

[18]B. M. Gorbovitskii and V. I. Perel', Zh. Eksp. Teor. Fiz. **85**, 1812 (1983) [Sov. Phys. JETP **58**, 1054 (1983)].
[19]R. Freedman and D. R. Fredkin, Phys. Rev. B **11**, 4847 (1975); S. S. Nedorezov, Kvantovye magnitnye i razmernye yavleniya v metallakh so slozhnoi poverkhnost'yu Fermi (Quantum Magnetic and Dimensional Phenomena in Metals with a Complex Fermi Surface), Doctoral Dissertation (Author's abstract), Physico-Technical Low Temperature Institute, USSR Academy of Sciences (FTINT AN SSSR), Kharkov (1985).
[20]A. Erdélyi *et al.*, *Higher Transcendental Functions*, Vol. 2, McGraw-Hill, New York (1953); M. Abramowitz and I. M. Stegun, *Handbook of Mathematical Functions*, Dover, New York (1965).
[21]N. E. Alekseevskii and V. I. Nizhankovskii, *Elektrony provodimosti (Conduction Electrons)*, Nauka, Moscow (1985), p. 197.
[22]B. I. Kochelaev and Yu. N. Proshin, Fiz. Tverd. Tela (Leningrad) **27**, 265 (1985) [Sov. Phys. Solid State **27**, 161 (1985)].
[23]A. Stesmans and J. Witters, Phys. Rev. B **23**, 3159 (1981).
[24]S. Oseroff, B. L. Gehman, and S. Schultz, Phys. Rev. B **15**, 1291 (1977); R. P. Notley, J. R. Sambles, and J. E. Cousins, Solid State Phys. **25**, 1125 (1978).

Translated by M. Damashek